Journal of Quantitative Spectroscopy & Radiative Transfer 163 (2015) 39–49

Contents lists available at ScienceDirect

Journal of Quantitative Spectroscopy & Radiative Transfer

journal homepage: www.elsevier.com/locate/jqsrt

Semi-empirical studies of atomic transition probabilities, oscillator strengths and radiative lifetimes in Hf II

S. Bouazza [a,*], P. Quinet [b,c], P. Palmeri [b]

[a] LISM, E. A. 4695 Université de Reims-Champagne-Ardenne, UFR SEN, BP 1039, F-51687 Reims Cedex 2, France
[b] Astrophysique et Spectroscopie, Université de Mons, B-7000 Mons, Belgium
[c] IPNAS, Université de Liège, B-4000 Liège, Belgium

ARTICLE INFO

Article history:
Received 27 February 2015
Accepted 21 April 2015
Available online 30 April 2015

Keywords:
Atomic structure
Transition probabilities
Oscillator strengths
Lifetimes
Hf II spectrum

ABSTRACT

Over the past few years, laser induced fluorescence and Fourier Transform techniques have been applied to measure radiative lifetimes and branching fractions in Hf II in order to derive oscillator strengths and transition probabilities. In the present work, we propose to compare for the first time these experimental data to computed values obtained by two different semi-empirical approaches, respectively based on a parametrization of the oscillator strengths and on a pseudo-relativistic Hartree–Fock model including core-polarization effects. The overall agreement between all sets of data is found to be good. We furthermore give radial integrals of the main atomic transitions in this study: $\langle 5d6s6p|r^1|5d^26s\rangle = 0.1504$ (0.0064), $\langle 6s^26p|r^1|5d6s^2\rangle = 1.299$ (0.012), $\langle 5d^26p|r^1|5d^26s\rangle = -0.298$ (0.013), $\langle 5d^26p|r^1|5d^3\rangle = 2.025$ (0.027). Finally a new set of oscillator strengths and transition probabilities is reported for many transitions in Hf II.

1. Introduction

It is very interesting to study atomic and nuclear properties of refractory elements with $Z = 71–78$ and particularly hafnium which has the longest known isotopic chain of 31 isotopes. High-resolution Doppler limited laser spectroscopy has been employed in the past for example to investigate hyperfine structure of selected lines of hafnium in the red spectral region. Using laser induced fluorescence and optogalvanic detection methods, measurements were performed in the plasma of a liquid nitrogen cooled hollow cathode discharge in the atomic spectrum of hafnium [1,2]. Nevertheless our measurements have been limited to low-lying levels due to the high evaporation temperature of this refractory element. Today the development of various methods for producing intense atomic beams and the introduction of Fourier transform and laser spectroscopic techniques have considerably improved ability for performing any kinds of measurements on refractory elements. Radiative lifetimes, for instance, from laser-induced fluorescence measurements, reaching an accuracy of 5% were reported for 41 odd-parity levels of Hf II. These lifetimes were combined with branching fractions measured using Fourier transform spectrometry and transition probabilities for 150 lines of Hf II were determined [3]. In another work new and improved radiative lifetimes for eight levels in Hf I and eighteen levels in Hf II, along with oscillator strengths and wavelengths for 195 transitions in Hf II, were presented [4]. Besides these experimental works unfortunately no huge number of theoretical calculations were achieved in the same time like in the case of other ions. For instance the spectrum and extended term analysis of Hf II is limited to two low-lying configurations for odd- and three ones for even-parity levels up to now. The very interesting Kurucz semi-empirical evaluations for oscillator strength,

* Corresponding author.
E-mail address: safa.bouazza@univ-reims.fr (S. Bouazza).

http://dx.doi.org/10.1016/j.jqsrt.2015.04.013
0022-4073/

lifetimes or atomic transition probabilities are not yet inserted as regards Hf II in his famous Tables [5]. We propose then to bring our contributions in order to fill up at least partially this lack of theoretical background.

It is worth reminding the astrophysical interest of a reliable knowledge of radiative parameters in lowly ionization stages of hafnium. Indeed, this element has recently been proposed to be used as a stable reference element in nucleocosmochronometry based on the unstable elements thorium and uranium whose radioactive decay timescales are well known [4]. In this latter study, it was also shown that newly Hf abundances in the Sun and 10 metal poor, r-process-rich halo stars set the stage for improved radioactive stellar age determinations using the Th/Hf chronometer pair. In addition, the observed stellar abundance ratio of Hf/Eu was found to be larger than previous estimates of the solar system r-process-only value, suggesting a somewhat larger contribution from the r-process to the production of hafnium.

2. Oscillator strength and transition probability determination in Hf II

2.1. Oscillator strength parametrization method

In this study we looked first into electric dipole transitions. We had recourse to a semi-empirical method for parametrization of oscillator strengths. The complete details of this method were already described in previous paper [6]; nevertheless let us mention once more that we transformed angular coefficients of the transition matrix from SL coupling to intermediate one, using fine structure eigenvector amplitudes, previously determined [7–9] and presently reanalyzed for odd-parity ones.

For the electric dipole transitions, the weighted oscillator strength *gf* is related to the line strength **S** [10]:

$$gf = 8\,\pi^2\, m\, c\, a_0^2\, \frac{\sigma}{3h}\,\mathbf{S} = 303.76 \times 10^{-8}\,\sigma\,\mathbf{S}, \tag{1}$$

where a_0 is the Bohr radius, $\sigma = |E(\gamma) - E(\gamma')|/hc$ and h is Planck's constant. Let us point out that $E(\gamma)$ is the energy of the initial state. The quantities with primes refer to the final state.

The electric dipole line strength is defined by

$$\mathbf{S} = \left| \left\langle \gamma J \middle\| \mathbf{P^1} \middle\| \gamma' J' \right\rangle \right|^2, \tag{2}$$

The tensorial operator $\mathbf{P^1}$ in the reduced matrix element represents the electric dipole moment.

For a multiconfiguration system, the wavefunctions $|\gamma J\rangle$ and $|\gamma' J'\rangle$ are expanded in terms of a set of basis functions $|\psi\, SLJ\rangle$ and $|\psi'\, S'L'J'\rangle$, respectively:

$$|\gamma J\rangle = \sum_i c_i |\psi SLJ\rangle,\ |\gamma' J'\rangle = \sum_j c'_j |\psi' S'L'J'\rangle \tag{3}$$

The square root of the line strength may be written in the following form:

$$S_{\gamma\gamma'}^{1/2} = \sum_i \sum_j c_i c'_j \left\langle \psi SLJ \middle\| \mathbf{P}^1 \middle\| \psi' S'L'J' \right\rangle \tag{4}$$

From Eqs. (2) and (5), we can express the *gf*-value as a linear combination:

$$(gf)^{1/2} = \sum\nolimits_{nl,n'l'} (303.76\,\sigma \times 10^{-8})^{1/2} \times \sum\nolimits_i \sum\nolimits_j c_i c'_j \left\langle \psi SLJ \middle\| \mathbf{P}^1 \middle\| \psi' S'L'J' \right\rangle, \tag{5}$$

where the sum is over all possible transitions (ns↔n′p, nd↔n′p, nd↔n′f)

The weighted transition probability is [10]

$$gA = (2j'+1)A = 64\,\pi^4\, e^2\, a\, \sigma^3\, \mathbf{S}/3h = 2.0261 \times 10^{-6}\sigma^3\, \mathbf{S} \tag{6}$$

where σ is given in cm^{-1} and **S** in atomic units of $e^2 a_0^2$.

Using Eqs. (1) and (6) one obtains, in s^{-1}:

$$gA = 0.66702\,\sigma^2\, gf \tag{7}$$

The extended basis system for odd-parity configurations used in this analysis corresponds to the 6 following configurations: $5d^2 6p$, 5d6s6p, $6s^2 6p$, $5d^2 7p$, 5d6s7p, $6s^2 7p$ where configuration mixing is expected to be very strong between the three first cited configurations. Regarding even-parity configurations were involved: $5d^1 6s^2$, $5d^2 6s^1$, $5d^3$, $5d^1 6s^1 7s^1$, $5d^2 7s^1$, $5d^2 6d^1$ and $5d^2 8s^1$. As it is commonly the case with the 5d-elements, Hf II has many low-lying levels below 40,000 cm^{-1} which are members of the even-parity configurations as well as the odd-parity ones.

Unfortunately due to a small number of experimental energy levels, available in literature only for the two low configurations of this basis system, we fixed the 3 last odd-parity configuration fine structure parameter values to their weighted *ab-initio* data, computed by means of Cowan code [10]. The fitted fine structure parameter values of this extended basis system are shown in Table 1. Transition integrals, treated as free parameters in the least squares fit

Table 1
Fine structure parameter values adopted in the oscillator strength parametrization method. All values are given in cm^{-1}.

Configuration	5d6s6p	$6s^2 6p$	$5d^2 6p$
E_{av}	41,980 (175)	43,002 (527)	50,497 (59)
$F^2(5d,5d)$			35,093 (751)
$F^4(5d,5d)$			20,016 (1013)
$F^2(5d,6p)$	16,009 (627)		13,995 (387)
$G^1(6s,6p)$	20,115 (920)		
$G^2(5d,6s)$	15,849 (980)		
$G^1(5d,6p)$	8811 (302)		8350 (187)
$G^3(5d,6p)$	4502 (928)		3398 (541)
ζ_{5d}	1668 (68)		1424 (39)
ζ_{6p}	4180 (130)	4476 (310)	3426 (102)
α	−14 (7)		−14 (7)
β	−41 (38)		−41 (38)
Configuration interaction parameters			
	$6s^2 6p$–$5d^2 6p$	5d6s6p–$6s^2 6p$	5d6s6p–$5d^2 6p$
D^2(6s6s, 5d5d)	18,395 (602)		
D^2(5d6p,6s6p)		−15,745 (707)	
E^1(5d6p,6s6p)		−14,441 (477)	
D^2(6s6p, 5d6p)			−12,920 (321)
E^1(6s6p, 6p5d)			−11,878 (238)
D^2(5d6s, 5d5d)			−20,488 (397)

to experimental oscillator strength (*gf*) values, were then extracted; we give the main deduced values in Table 2. The values of the six remaining integrals although predicted by theory but expected to be small in this study were fixed to zero and then are not listed in this Table 2.

Table 2
Transition radial integrals obtained in the fitting procedure used in the oscillator strength parametrization method.

Transition	Value	Uncertainty
⟨5d6s6p |r[1]| 5d6s[2]⟩	−0.267	0.011
⟨5d6s6p |r[1]| 5d[2]6s⟩	0.1504	0.0064
⟨5d6s6p |r[1]| 5d6s7s⟩	0.123	0.009
⟨6s[2]6p |r[1]| 5d6s[2]⟩	1.299	0.012
⟨5d[2]6p |r[1]| 5d[2]6s⟩	−0.298	0.013
⟨5d[2]6p |r[1]| 5d[3]⟩	2.025	0.027
⟨5d[2]6p |r[1]| 5d[2]7s⟩	−0.135	0.009
⟨5d[2]6p |r[1]| 5d[2]6d⟩	0.641	0.026
⟨5d[2]6p |r[1]| 5d[2]8s⟩	−0.038	0.015
⟨5d6s7p |r[1]| 5d6s[2]⟩	−0.069	0.030
⟨5d6s7p |r[1]| 5d[2]6s⟩	−0.023	0.015
⟨5d6s7p |r[1]| 5d6s7s⟩	−0.37	0.03

Table 3
Optimized radial parameter values (in cm^{-1}) adopted in the HFR+CPOL method.

Configuration	Parameter	Ab initio value	Fitted value	Ratio
Even parity				
$5d6s^2$	E_{av}	9213	9842	
	ζ_{5d}	1833	1528	0.834
$5d^3$	E_{av}	30,110	30,588	
	$F^2(5d,5d)$	43,338	33,392	0.769
	$F^4(5d,5d)$	27,936	19,782	0.708
	ζ_{5d}	1468	1207	0.822
$5d^26s$	Eav	14,747	14,921	
	$F^2(5d,5d)$	46,353	36,336	0.784
	$F^4(5d,5d)$	30,087	21,182	0.704
	ζ_{5d}	1645	1363	0.828
	$G^2(5d,6s)$	20,915	18,287	0.874
Odd parity				
$5d^26p$	E_{av}	48,896	51,067	
	$F^2(5d,5d)$	47,606	37,187	0.781
	$F^4(5d,5d)$	30,993	21,859	0.705
	ζ_{5d}	1715	1508	0.879
	ζ_{6p}	2611	3224	1.235
	$F^2(5d,6p)$	19,038	14,554	0.764
	$G^1(5d,6p)$	11,327	8943	0.790
	$G^3(5d,6p)$	8343	5048	0.605
5d6s6p	E_{av}	40,857	43,030	
	ζ_{5d}	1895	1626	0.858
	ζ_{6p}	3172	4218	1.330
	$F^2(5d,6p)$	20,338	16,186	0.796
	$G^2(5d,6s)$	20,628	17,568	0.852
	$G^1(5d,6p)$	11,351	10,056	0.886
	$G^3(5d,6p)$	8600	5340	0.621
	$G^1(6s,6p)$	33,422	23,379	0.700
$6s^26p$	E_{av}	44,825	46,283	
	ζ_{6p}	3812	4756	1.2476
$5d^26p$–5d6s6p	$D^2(5d5d,5d6s)$	−25,393	−20,032	0.789
	$D^2(5d6p,6s6p)$	−19,110	−15,075	0.789
	$E^1(5d6p,6s6p)$	−18,845	−14,866	0.789
$5d^26p$–$6s^26p$	$D^2(5d5d,6s6s)$	23,298	25,865	1.110
5d6s6p–$6s^26p$	$D^2(5d6p,6s6p)$	−19,733	−13,863	0.703
	$E^1(5d6p,6s6p)$	−19,274	−13,541	0.703

2.2. *Pseudo-relativistic Hartree–Fock method with core-polarization corrections*

In the present work, we also used the pseudo-relativistic Hartree–Fock (HFR) approach of Cowan [10] in which we have incorporated core-polarization effects by means of a model potential and a correction to the dipole operator (HFR+CPOL: see e.g. [11,12]). In a previous work on the isoelectronic ion Ta III [13], an excellent agreement was obtained between HFR+CPOL lifetimes and the accurate values measured by time-resolved laser-induced-fluorescence spectroscopy. We have adopted the same physical model here considering a set of 43 configurations: $5d6s^2+5d^3+5d^26s+5d^26d+5d6p^2+5d6d^2+5d5f^2+5d6f^2+5d6s6d+5d6p5f+5d6p6f+5d5f6f+6s^26d+6s6p^2+6p^26d+6s6d^2+6d^3+6s5f^2+6d5f^2+6s6f^2+6d6f^2$ (even parity)

Table 4
Comparison between available experimental radiative lifetimes and the results obtained in the present work using the HFR+CPOL model. All values are given in ns.

E (cm^{-1})	J	Lundqvist et al. [3]	Lawler et al. [4]	HFR+CPOL
28,068.79	1.5		39.4 ± 2.0	37.5
29,160.04	0.5		43.8 ± 2.2	44.6
29,405.12	2.5	29.7 ± 2.4	26.4 ± 1.3	24.4
31,784.16	1.5	21.8 ± 1.8	18.9 ± 0.9	19.3
33,136.20	0.5		17.6 ± 0.9	18.0
33,180.92	2.5	18.1 ± 1.5	16.3 ± 0.8	15.4
33,776.24	3.5	34.8 ± 2.5	32.4 ± 1.6	32.4
34,123.93	1.5	24.5 ± 2.5	23.3 ± 1.2	17.5
34,355.13	2.5	16.2 ± 1.4	14.7 ± 0.7	13.0
34,942.36	2.5	8.4 ± 0.5	8.0 ± 0.4	7.1
36,373.42	1.5		17.7 ± 0.9	19.0
36,882.49	3.5		16.7 ± 0.8	18.8
37,885.90	1.5		3.4 ± 0.2	3.5
38,185.67	4.5		47.2 ± 2.4	56.5
38,398.56	0.5		28.3 ± 1.4	30.9
38,498.53	3.5	5.1 ± 0.3	5.0 ± 0.3	4.1
38,578.63	2.5		5.2 ± 0.3	4.5
39,226.46	1.5		29.1 ± 1.5	28.3
40,506.86	2.5		12.4 ± 0.6	10.6
41,406.86	3.5		5.2 ± 0.3	4.1
41,761.24	2.5		2.9 ± 0.2	2.7
42,391.09	4.5		4.2 ± 0.2	3.4
42,518.10	1.5	2.3 ± 0.2	2.15 ± 0.20	1.9
42,770.56	1.5	2.6 ± 0.2	2.6 ± 0.2	2.3
43,044.26	0.5	1.8 ± 0.2	1.75 ± 0.20	1.4
43,680.75	2.5	3.3 ± 0.2	3.2 ± 0.2	2.0
43,900.56	2.5		2.7 ± 0.2	4.1
44,399.96	3.5		4.1 ± 0.2	2.3
44,690.72	3.5		2.7 ± 0.2	4.4
45,643.25	0.5	2.2 ± 0.2	2.40 ± 0.2	2.1
46,124.89	4.5		2.8 ± 0.2	2.4
46,209.05	5.5		3.3 ± 0.2	2.8
46,495.37	0.5	2.7 ± 0.2	2.7 ± 0.2	2.4
46,674.36	1.5	2.1 ± 0.2	2.00 ± 0.20	1.8
47,157.57	3.5		3.2 ± 0.2	2.7
47,904.39	2.5	2.0 ± 0.2	2.05 ± 0.20	1.9
47,973.56	1.5		2.50 ± 0.20	2.1
48,930.75	3.5		2.10 ± 0.20	1.7
49,005.64	2.5		2.6 ± 0.20	2.0
49,840.47	4.5	3.1 ± 0.2	3.1 ± 0.2	2.6
52,340.08	3.5	1.9 ± 0.2		1.6
53,227.27	3.5		2.55 ± 0.20	2.1

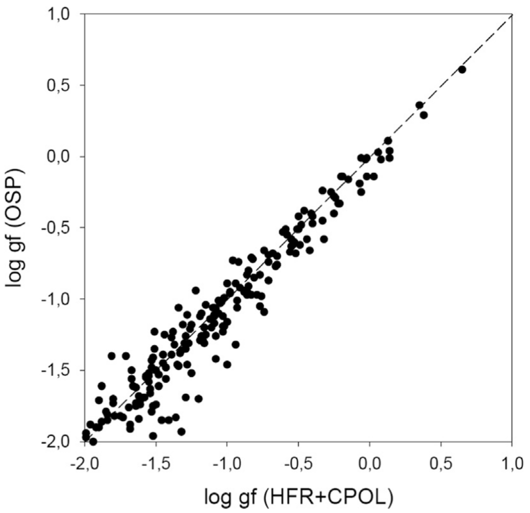

Fig. 1. Comparison between the log *gf*-values obtained in the present work with the oscillator strength parametrization method (OSP) and the pseudo-relativistic Hartree–Fock approach including core-polarization effects (HFR+CPOL). Only transitions with log $gf > -2$ are shown in the figure.

and $5d^26p+5d^25f+5d^26f+5d6s6p+5d6s5f+5d6s6f+5d6p6d+5d6d5f+5d6d6f+6s^26p+6s^25f+6s^26f+6p^25f+6p^26f+6p^3+6p6d^2+6d^25f+6d^26f+6p5f^2+6p6f^2+5f^26f+5f6f^2$ (odd parity). For the core-polarization corrections, we considered an erbium – like core surrounded by 3 valence electrons. The adopted dipole polarizabilty was $\alpha_d = 3.85\ a_0^3$ which corresponds to a Hf V ionic core [14]. The cut-off radius used was the HFR mean radius of the outermost core orbital 5p, i.e. $r_c = 1.33\ a_0$. To optimize the calculation of oscillator strengths, the HFR+CPOL method was combined with a semi-empirical fitting of the radial parameters minimizing the discrepancies between the computed energies and the experimental values compiled at the National Institute of Standards and Technology (NIST) [15] for the $5d6s^2$, $5d^3$ and $5d^26s$ even-parity configurations and published by Wyart and Blaise [8] for the $5d^26p$, 5d6s6p and $6s^26p$ odd-parity configurations. The adopted values for the radial parameters are reported in Table 3. At the end of the fitting process, the average deviations between experimental and computed energy levels were found to be equal to 118 cm^{-1} (even parity) and 140 cm^{-1} (odd parity). These calculations can be seen as an extension of our previous similar works on singly ionized 5d-transition atoms Ta II [16], W II [17], Re II [18], Os II [19], Ir II [20], Pt II [21], and Au II [22].

3. Results and discussion

In Table 4, we give the oscillator strengths computed in the present work using both methods described here above for a sample of about 300 selected Hf II transitions. More precisely, only lines with HFR+CPOL log *gf*-values greater than −1.0 are listed in this table in which are also reported the available experimental data [3,4]. When comparing the results obtained with our two computational approaches, one can notice an overall good agreement (within 20–30%). This general agreement is illustrated in Fig. 1 where oscillator strengths are compared for all transitions with log $gf > -2.0$. It is not worth making the comparison for weaker transitions since most of them were found to be affected by large cancellation effects in the HFR+CPOL line strength calculations, indicating that those results could be affected by large uncertainties.

When looking at Table 4, we also note that the agreement between the oscillator strengths computed in the present work and the available experimental data is satisfactory, all sets of data standing within 30% for most transitions. Much larger differences are nevertheless observed for some lines, in particular for those situated at 2288.632, 2677.555 and 4245.845 Å for which the discrepancies between the HFR+CPOL *gf*-values and the experimental data [3] can reach several orders of magnitude. However, it is interesting to note that, for the same transitions, the results obtained in our work using the oscillator strength parametrization method show similar discrepancies with experiment.

Finally, in Table 5, we report on the comparison between our HFR+CPOL radiative lifetimes and the accurate experimental values recently measured using laser-induced fluorescence spectroscopy by Lundqvist et al. [3] and Lawler et al. [4]. As seen from this table, a very good agreement is also observed, the ratios $\tau_{HFR+CPOL}/\tau_{EXP}$ being found to be equal to 0.84 ± 0.08 and 0.93 ± 0.19 when considering the experimental lifetimes from [3] and [4], respectively.

4. Conclusion

Very interesting experimental data of Hf II lifetimes, transition probabilities and oscillator strengths were given some years ago but unfortunately without any theoretical background. In the present work we have compared these experimental values with computed ones obtained using two independent semi-empirical methods. We have confirmed the well-founded basis of these experimental sets of data. In many analyses of physical and astrophysical problems linked to fundamental characteristics of atomic and ionic excited states, a large number of radial transition integrals are required. Such parameters are given in this paper for the twelve main Hf II transition arrays. Despite the scarcity of Hf II energy levels, their eigenvector amplitudes could nevertheless be used to determine the angular part of the matrix element: $\langle \psi SLJ \| \mathbf{P^1} \| \psi' S'L'J' \rangle$ (see Eq. (5)), recurring to Racah Algebra as in the cases of hyperfine structure and isotope shift studies. As for the latter fields we have to confess that we prefer to have at our disposal more experimental energy levels and then more accurate eigenvectors and less oscillator strength values than the opposite situation as in the case of Hf II. We have to point out, according to our knowledge that all these transition radial integral values are given for the first time. Finally our investigation of singly ionized hafnium was extended by comparing our calculated oscillator strengths with available experimental data and by predicting new values for a rather large number of transitions. We hope that this work, in the image of our previous studies [16–24], will constitute a good stimulus and a

Table 5
Oscillator strengths for selected transitions (log *gf* (HFR+CPOL) > −1.0) in Hf II.

λ (Å)[a]	Lower level[b]			Upper level[b]			log *gf* Experiment		log *gf* [c] This work	
	E (cm^{-1})		*J*	*E* (cm^{-1})		*J*	[3]	[4]	OSP	HFR+CPOL
1774.757	0	(e)	1.5	56,346	(o)	1.5				−0.23
1815.640	0	(e)	1.5	55,077	(o)	1.5				−0.97
1815.985	3051	(e)	2.5	58,117	(o)	2.5				−0.96
1869.365	0	(e)	1.5	53,494	(o)	1.5				−0.84
1919.518	0	(e)	1.5	52,096	(o)	0.5				−0.61
1922.111	3051	(e)	2.5	55,077	(o)	1.5				−0.71
1922.727	3051	(e)	2.5	55,060	(o)	2.5				−0.23
1955.662	0	(e)	1.5	51,134	(o)	1.5				−0.90
1963.804	3051	(e)	2.5	53,972	(o)	3.5				−0.79
1964.242	0	(e)	1.5	50,910	(o)	2.5				−0.05
1993.799	4905	(e)	2.5	55,060	(o)	2.5				−0.85
2012.776	3051	(e)	2.5	52,717	(o)	1.5				−0.52
2028.195	3051	(e)	2.5	52,340	(o)	3.5	−0.334		−0.14	−0.19
2088.791	3051	(e)	2.5	50,910	(o)	2.5				−0.74
2107.476	4905	(e)	2.5	52,340	(o)	3.5	−0.915		−0.69	−0.71
2156.435	6344	(e)	3.5	52,703	(o)	2.5				−0.97
2178.923	3051	(e)	2.5	48,931	(o)	3.5				−0.38
2212.463	8362	(e)	4.5	53,546	(o)	4.5				−0.72
2254.000	3645	(e)	1.5	47,996	(o)	0.5				−0.32
2255.166	3645	(e)	1.5	47,974	(o)	1.5				−0.71
2257.897	12,070	(e)	2.5	56,346	(o)	1.5				−0.67
2266.529	3051	(e)	2.5	47,158	(o)	3.5				−0.99
2266.832	4905	(e)	2.5	49,006	(o)	2.5				−0.31
2273.153	8362	(e)	4.5	52,340	(o)	3.5	−0.628		−0.58	−0.32
2277.172	0	(e)	1.5	43,901	(o)	2.5				−0.73
2284.592	14,359	(e)	1.5	58,117	(o)	2.5				−0.54
2288.632	0	(e)	1.5	43,681	(o)	2.5	−2.544		−0.62	−0.49
2321.158	4905	(e)	2.5	47,974	(o)	1.5				−0.32
2322.477	0	(e)	1.5	43,044	(o)	0.5	−0.140		−0.14	−0.02
2323.262	3645	(e)	1.5	46,674	(o)	1.5	−0.550		−0.58	−0.44
2324.514	12,070	(e)	2.5	55,077	(o)	1.5				−0.42
2324.892	4905	(e)	2.5	47,904	(o)	2.5	−0.315		−0.45	−0.33
2332.967	3645	(e)	1.5	46,495	(o)	0.5	−0.946		−0.85	−0.81
2343.327	6344	(e)	3.5	49,006	(o)	2.5				−0.07
2347.448	6344	(e)	3.5	48,931	(o)	3.5				−0.07
2351.220	0	(e)	1.5	42,518	(o)	1.5	−0.331		−0.16	−0.15
2371.414	12,921	(e)	1.5	55,077	(o)	1.5				−0.79
2372.351	12,921	(e)	1.5	55,060	(o)	2.5				−0.95
2380.306	3645	(e)	1.5	45,643	(o)	0.5	−0.513		−0.66	−0.42
2381.002	14,359	(e)	1.5	56,346	(o)	1.5				−0.33
2393.185	12,921	(e)	1.5	54,694	(o)	2.5				−0.05
2393.362	4905	(e)	2.5	46,674	(o)	1.5	−0.136		−0.25	−0.06
2393.836	0	(e)	1.5	41,761	(o)	2.5				−0.30
2400.815	3051	(e)	2.5	44,691	(o)	3.5				−0.55
2403.609	13,486	(e)	2.5	55,077	(o)	1.5				−0.84
2404.572	13,486	(e)	2.5	55,060	(o)	2.5				−0.27

Table 5 (*continued*)

λ (Å)[a]	Lower level[b]			Upper level[b]			log *gf* Experiment		log *gf* [c] This work	
	E (cm^{-1})		*J*	*E* (cm^{-1})		*J*	[3]	[4]	OSP	HFR+CPOL
2405.425	6344	(e)	3.5	47,904	(o)	2.5	0.052		−0.14	0.03
2406.447	11,952	(e)	0.5	53,494	(o)	1.5				−0.18
2410.142	8362	(e)	4.5	49,840	(o)	4.5	0.024		0.04	0.14
2413.347	12,070	(e)	2.5	53,494	(o)	1.5				−0.63
2415.962	11,952	(e)	0.5	53,331	(o)	0.5				−0.85
2417.699	3051	(e)	2.5	44,400	(o)	3.5				−0.97
2425.978	13,486	(e)	2.5	54,694	(o)	2.5				−0.22
2428.994	12,070	(e)	2.5	53,227	(o)	3.5				−0.34
2433.575	17,369	(e)	2.5	58,448	(o)	3.5				0.25
2434.772	17,389	(e)	4.5	58,448	(o)	3.5				−0.63
2449.444	6344	(e)	3.5	47,158	(o)	3.5				−0.58
2452.296	11,952	(e)	0.5	52,717	(o)	1.5				−0.81
2453.333	17,369	(e)	2.5	58,117	(o)	2.5				0.15
2453.998	17,711	(e)	3.5	58,448	(o)	3.5				−0.56
2455.198	14,359	(e)	1.5	55,077	(o)	1.5				−0.64
2460.499	3051	(e)	2.5	43,681	(o)	2.5	−0.254		0.03	0.06
2463.938	12,921	(e)	1.5	53,494	(o)	1.5				−0.50
2464.192	8362	(e)	4.5	48,931	(o)	3.5				0.32
2465.070	15,084	(e)	3.5	55,639	(o)	4.5				−0.26
2469.188	13,486	(e)	2.5	53,972	(o)	3.5				0.13
2473.914	12,921	(e)	1.5	53,331	(o)	0.5				−0.30
2478.542	14,359	(e)	1.5	54,694	(o)	2.5				−0.91
2481.437	17,830	(e)	1.5	58,117	(o)	2.5				−0.55
2483.357	3645	(e)	1.5	43,901	(o)	2.5				−0.97
2496.993	3645	(e)	1.5	43,681	(o)	2.5	−0.581		−0.55	−0.58
2500.741	15,084	(e)	3.5	55,060	(o)	2.5				−0.30
2512.699	4905	(e)	2.5	44,691	(o)	3.5				−0.64
2512.965	12,921	(e)	1.5	52,703	(o)	2.5				0.04
2513.035	6344	(e)	3.5	46,125	(o)	4.5				0.11
2515.491	13,486	(e)	2.5	53,227	(o)	3.5				0.01
2516.886	3051	(e)	2.5	42,771	(o)	1.5	0.039		−0.01	0.14
2521.484	17,830	(e)	1.5	57,478	(o)	0.5				−0.22
2531.198	4905	(e)	2.5	44,400	(o)	3.5				0.02
2548.181	13,486	(e)	2.5	52,717	(o)	1.5				−0.34
2551.391	17,389	(e)	4.5	56,572	(o)	5.5				0.48
2551.434	11,952	(e)	0.5	51,134	(o)	1.5				−0.25
2551.853	12,921	(e)	1.5	52,096	(o)	0.5				−0.97
2559.191	12,070	(e)	2.5	51,134	(o)	1.5				−0.40
2570.704	15,084	(e)	3.5	53,972	(o)	3.5				−0.60
2571.679	3645	(e)	1.5	42,518	(o)	1.5	−0.071		−0.19	−0.07
2572.942	13,486	(e)	2.5	52,340	(o)	3.5	−1.154		−3.03	−0.85
2573.910	12,070	(e)	2.5	50,910	(o)	2.5				0.19
2576.826	8362	(e)	4.5	47,158	(o)	3.5				−0.13
2578.149	4905	(e)	2.5	43,681	(o)	2.5	−0.617		−0.33	−0.22
2582.515	3051	(e)	2.5	41,761	(o)	2.5				−0.71
2595.588	17,830	(e)	1.5	56,346	(o)	1.5				−0.84
2599.198	15,084	(e)	3.5	53,546	(o)	4.5				−0.74

2606.377	3051	(e)	2.5	41,407	(o)	3.5				−0.35
2607.248	14,359	(e)	1.5	52,703	(o)	2.5				−0.32
2613.616	17,389	(e)	4.5	55,639	(o)	4.5				0.35
2614.295	15,254	(e)	0.5	53,494	(o)	1.5				−0.86
2620.930	15,084	(e)	3.5	53,227	(o)	3.5				−0.87
2622.747	3645	(e)	1.5	41,761	(o)	2.5				−0.23
2626.949	6344	(e)	3.5	44,400	(o)	3.5				0.16
2635.783	17,711	(e)	3.5	55,639	(o)	4.5				−0.30
2638.718	0	(e)	1.5	37,886	(o)	1.5		−0.17	−0.40	−0.25
2641.410	8362	(e)	4.5	46,209	(o)	5.5		0.57	0.61	0.65
2647.297	8362	(e)	4.5	46,125	(o)	4.5				0.30
2649.132	14,359	(e)	1.5	52,096	(o)	0.5				−0.78
2651.159	17,369	(e)	2.5	55,077	(o)	1.5				−0.08
2657.488	15,084	(e)	3.5	52,703	(o)	2.5				−0.62
2657.847	4905	(e)	2.5	42,518	(o)	1.5	−0.902		−0.96	−0.85
2661.883	6344	(e)	3.5	43,901	(o)	2.5				−0.66
2665.977	12,921	(e)	1.5	50,419	(o)	1.5				−0.36
2671.240	13,486	(e)	2.5	50,910	(o)	2.5				−0.68
2676.607	17,711	(e)	3.5	55,060	(o)	2.5				−0.82
2677.555	6344	(e)	3.5	43,681	(o)	2.5	−1.866		−1.05	−0.77
2678.398	17,369	(e)	2.5	54,694	(o)	2.5				−0.79
2683.358	15,084	(e)	3.5	52,340	(o)	3.5	0.319		0.36	0.35
2685.208	17,830	(e)	1.5	55,060	(o)	2.5				−0.35
2706.643	12,070	(e)	2.5	49,006	(o)	2.5				−0.69
2706.735	13,486	(e)	2.5	50,419	(o)	1.5				−0.43
2711.929	17,830	(e)	1.5	54,694	(o)	2.5				−0.52
2712.143	12,070	(e)	2.5	48,931	(o)	3.5				−0.92
2712.430	4905	(e)	2.5	41,761	(o)	2.5				−0.65
2718.494	14,359	(e)	1.5	51,134	(o)	1.5				−0.73
2731.164	17,369	(e)	2.5	53,972	(o)	3.5				−0.76
2732.671	17,389	(e)	4.5	53,972	(o)	3.5				−0.83
2738.765	4905	(e)	2.5	41,407	(o)	3.5				0.00
2751.811	8362	(e)	4.5	44,691	(o)	3.5				−0.38
2756.913	17,711	(e)	3.5	53,972	(o)	3.5				−0.13
2770.439	12,921	(e)	1.5	49,006	(o)	2.5				−0.99
2772.332	14,359	(e)	1.5	50,419	(o)	1.5				−0.53
2773.356	6344	(e)	3.5	42,391	(o)	4.5		0.30	0.29	0.38
2773.508	11,952	(e)	0.5	47,996	(o)	0.5				−0.56
2774.014	8362	(e)	4.5	44,400	(o)	3.5				−0.45
2786.300	15,254	(e)	0.5	51,134	(o)	1.5				−0.83
2789.495	17,389	(e)	4.5	53,227	(o)	3.5				−0.05
2789.710	17,711	(e)	3.5	53,546	(o)	4.5				0.26
2789.828	12,070	(e)	2.5	47,904	(o)	2.5	−0.923		−0.74	−0.71
2808.003	4905	(e)	2.5	40,507	(o)	2.5				−0.64
2813.872	3051	(e)	2.5	38,579	(o)	2.5				−0.84
2814.480	13,486	(e)	2.5	49,006	(o)	2.5				−0.19
2814.760	17,711	(e)	3.5	53,227	(o)	3.5				−0.21
2816.059	17,830	(e)	1.5	53,331	(o)	0.5				−0.87
2820.231	3051	(e)	2.5	38,499	(o)	3.5	−0.044	−0.05	−0.02	0.08
2820.427	13,486	(e)	2.5	48,931	(o)	3.5				−0.75
2822.680	6344	(e)	3.5	41,761	(o)	2.5				−0.25
2828.135	17,369	(e)	2.5	52,717	(o)	1.5				−0.66
2829.325	17,369	(e)	2.5	52,703	(o)	2.5				−0.38
2849.212	12,070	(e)	2.5	47,158	(o)	3.5				−0.02

Table 5 (*continued*)

λ (Å)[a]	Lower level[b]			Upper level[b]			log *gf* Experiment		log *gf* [c] This work	
	E (cm^{-1})		*J*	*E* (cm^{-1})		*J*	[3]	[4]	OSP	HFR+CPOL
2850.152	12,921	(e)	1.5	47,996	(o)	0.5				−0.80
2851.210	6344	(e)	3.5	41,407	(o)	3.5				−0.58
2852.016	12,921	(e)	1.5	47,974	(o)	1.5				−0.48
2857.655	12,921	(e)	1.5	47,904	(o)	2.5	−0.850		−0.68	−0.68
2860.319	17,389	(e)	4.5	52,340	(o)	3.5	−0.500		−0.24	−0.33
2861.016	0	(e)	1.5	34,942	(o)	2.5	−0.693	−0.69	−0.63	−0.55
2861.702	3645	(e)	1.5	38,579	(o)	2.5				−0.13
2876.340	15,084	(e)	3.5	49,840	(o)	4.5	−0.062		−0.02	−0.03
2879.119	11,952	(e)	0.5	46,674	(o)	1.5	−1.107		−0.95	−0.98
2885.471	14,359	(e)	1.5	49,006	(o)	2.5				−0.72
2898.710	13,486	(e)	2.5	47,974	(o)	1.5				−0.33
2904.535	13,486	(e)	2.5	47,904	(o)	2.5	−0.947		−0.51	−0.59
2919.599	3645	(e)	1.5	37,886	(o)	1.5		−0.71	−0.70	−0.65
2929.638	0	(e)	1.5	34,124	(o)	1.5	−0.992	−0.94	−0.95	−0.86
2937.782	8362	(e)	4.5	42,391	(o)	4.5		−0.14	−0.01	−0.02
2960.806	17,369	(e)	2.5	51,134	(o)	1.5				−0.53
2961.798	12,921	(e)	1.5	46,674	(o)	1.5	−0.712		−0.53	−0.61
2967.237	11,952	(e)	0.5	45,643	(o)	0.5	−0.543		−0.51	−0.51
2968.803	4905	(e)	2.5	38,579	(o)	2.5				−0.39
2975.882	4905	(e)	2.5	38,499	(o)	3.5	−0.299	−0.27	−0.28	−0.25
2977.588	12,921	(e)	1.5	46,495	(o)	0.5	−0.911		−0.80	−0.85
2990.807	23,146	(e)	4.5	56,572	(o)	5.5				−0.96
3011.215	17,711	(e)	3.5	50,910	(o)	2.5				−0.55
3012.975	0	(e)	1.5	33,180	(o)	2.5	−0.681	−0.60	−0.62	−0.54
3025.286	8362	(e)	4.5	41,407	(o)	3.5				−0.72
3031.162	4905	(e)	2.5	37,886	(o)	1.5		−0.48	−0.47	−0.40
3046.024	15,084	(e)	3.5	47,904	(o)	2.5	−0.996		−0.87	−0.71
3055.414	15,254	(e)	0.5	47,974	(o)	1.5				−0.77
3064.689	12,070	(e)	2.5	44,691	(o)	3.5				−0.84
3080.635	17,389	(e)	4.5	49,840	(o)	4.5	0.083		0.11	0.13
3092.252	12,070	(e)	2.5	44,400	(o)	3.5				−0.79
3101.386	6344	(e)	3.5	38,579	(o)	2.5				−0.62
3109.113	6344	(e)	3.5	38,499	(o)	3.5	−0.288	−0.26	−0.29	−0.24
3110.877	14,359	(e)	1.5	46,495	(o)	0.5	−0.513		−0.68	−0.52
3134.725	3051	(e)	2.5	34,942	(o)	2.5	−0.458	−0.42	−0.42	−0.40
3140.770	12,070	(e)	2.5	43,901	(o)	2.5				−0.39
3176.855	4905	(e)	2.5	36,373	(o)	1.5		−0.80	−1.06	−0.93
3193.531	3051	(e)	2.5	34,355	(o)	2.5	−0.939	−0.89	−1.09	−0.74
3194.198	3645	(e)	1.5	34,942	(o)	2.5	−0.509	−0.49	−0.48	−0.48
3199.989	15,254	(e)	0.5	46,495	(o)	0.5	−0.629		−0.67	−0.56
3202.146	17,711	(e)	3.5	48,931	(o)	3.5				−0.96
3218.167	21,638	(e)	3.5	52,703	(o)	2.5				−0.79
3220.654	15,084	(e)	3.5	46,125	(o)	4.5				−0.37
3253.702	3051	(e)	2.5	33,776	(o)	3.5	−0.828	−0.81	−0.83	−0.77
3294.663	28,105	(e)	4.5	58,448	(o)	3.5				−0.93
3323.324	23,146	(e)	4.5	53,227	(o)	3.5				−0.35
3333.480	28,458	(e)	3.5	58,448	(o)	3.5				−0.93

3352.051	8362	(e)	4.5	38,186	(o)	4.5		−0.57	−0.77	−0.66
3358.289	17,389	(e)	4.5	47,158	(o)	3.5				−0.91
3370.662	28,458	(e)	3.5	58,117	(o)	2.5				−0.78
3376.671	15,084	(e)	3.5	44,691	(o)	3.5				−0.40
3389.829	3645	(e)	1.5	33,136	(o)	0.5		−0.78	−0.97	−0.79
3394.974	17,711	(e)	3.5	47,158	(o)	3.5				−0.20
3399.793	0	(e)	1.5	29,405	(o)	2.5	−0.612	−0.57	−0.60	−0.53
3407.757	12,070	(e)	2.5	41,407	(o)	3.5				−0.95
3469.265	15,084	(e)	3.5	43,901	(o)	2.5				−0.88
3478.980	17,389	(e)	4.5	46,125	(o)	4.5				−0.17
3487.573	17,830	(e)	1.5	46,495	(o)	0.5	−0.800			−0.78
3495.745	6344	(e)	3.5	34,942	(o)	2.5	−1.005	−0.97	−1.32	−0.94
3505.219	8362	(e)	4.5	36,882	(o)	3.5		−0.14	−0.33	−0.21
3511.862	28,105	(e)	4.5	56,572	(o)	5.5				−0.46
3518.740	14,359	(e)	1.5	42,771	(o)	1.5	−0.888		−0.94	−0.88
3535.649	4905	(e)	2.5	33,180	(o)	2.5			−0.76	−0.68
3561.659	0	(e)	1.5	28,069	(o)	1.5		−0.87	−0.97	−0.83
3569.034	6344	(e)	3.5	34,355	(o)	2.5	−0.514	−0.46	−0.58	−0.55
3599.110	18,898	(e)	1.5	46,674	(o)	1.5	−0.981		−0.89	−0.94
3599.305	27,285	(e)	1.5	55,060	(o)	2.5				−0.86
3600.052	20,135	(e)	2.5	47,904	(o)	2.5	−0.907		−0.92	−0.91
3644.352	6344	(e)	3.5	33,776	(o)	3.5	−0.657	−0.62	−0.76	−0.65
3659.032	17,369	(e)	2.5	44,691	(o)	3.5				−0.70
3661.045	15,084	(e)	3.5	42,391	(o)	4.5		−1.00	−0.71	−0.83
3661.738	17,389	(e)	4.5	44,691	(o)	3.5				−0.15
3665.349	11,952	(e)	0.5	39,226	(o)	1.5		−0.84	−0.97	−0.86
3699.731	13,486	(e)	2.5	40,507	(o)	2.5				−0.60
3718.769	30,595	(e)	1.5	57,478	(o)	0.5				−0.84
3719.276	4905	(e)	2.5	31,784	(o)	1.5	−0.850	−0.81	−0.91	−0.85
3737.869	18,898	(e)	1.5	45,643	(o)	0.5	−0.436		−0.51	−0.50
3744.969	23,146	(e)	4.5	49,840	(o)	4.5	−0.312		−0.25	−0.27
3745.763	17,711	(e)	3.5	44,400	(o)	3.5				−0.60
3758.021	28,458	(e)	3.5	55,060	(o)	2.5				−0.91
3762.507	31,878	(e)	4.5	58,448	(o)	3.5				0.27
3766.909	20,135	(e)	2.5	46,674	(o)	1.5	−0.206		−0.14	−0.20
3770.621	28,547	(e)	2.5	55,060	(o)	2.5				−0.87
3797.938	15,084	(e)	3.5	41,407	(o)	3.5				−0.82
3806.062	21,638	(e)	3.5	47,904	(o)	2.5	−0.031		−0.01	−0.06
3810.566	28,458	(e)	3.5	54,694	(o)	2.5				−0.26
3817.191	17,711	(e)	3.5	43,901	(o)	2.5				−0.14
3823.522	28,547	(e)	2.5	54,694	(o)	2.5				−0.78
3834.706	17,830	(e)	1.5	43,901	(o)	2.5				−0.96
3864.740	28,105	(e)	4.5	53,972	(o)	3.5				0.09
3877.098	23,146	(e)	4.5	48,931	(o)	3.5				−0.02
3882.227	30,595	(e)	1.5	56,346	(o)	1.5				−0.51
3900.627	30,942	(e)	5.5	56,572	(o)	5.5				−0.07
3917.447	21,638	(e)	3.5	47,158	(o)	3.5				−0.50
3923.902	12,921	(e)	1.5	38,399	(o)	0.5		−0.87	−1.01	−0.93
3935.632	17,369	(e)	2.5	42,771	(o)	1.5	−0.911		−0.96	−0.98
3945.331	32,778	(e)	2.5	58,117	(o)	2.5				−0.23
3979.379	28,105	(e)	4.5	53,227	(o)	3.5				−0.14
3984.841	28,458	(e)	3.5	53,546	(o)	4.5				−0.67
4007.357	28,547	(e)	2.5	53,494	(o)	1.5				−0.65
4047.959	30,942	(e)	5.5	55,639	(o)	4.5				0.34

Table 5 (*continued*)

λ (Å)[a]	Lower level[b]			Upper level[b]			log *gf* Experiment		log *gf*[c] This work	
	E (cm^{-1})		*J*	*E* (cm^{-1})		*J*	[3]	[4]	OSP	HFR+CPOL
4048.444	31,878	(e)	4.5	56,572	(o)	5.5				−0.81
4123.495	28,458	(e)	3.5	52,703	(o)	2.5				−0.60
4125.083	28,105	(e)	4.5	52,340	(o)	3.5	−0.953			−0.95
4127.789	14,359	(e)	1.5	38,579	(o)	2.5				−0.97
4162.405	17,389	(e)	4.5	41,407	(o)	3.5				−0.91
4177.520	17,830	(e)	1.5	41,761	(o)	2.5				−0.74
4232.426	18,898	(e)	1.5	42,518	(o)	1.5	−0.631		−0.42	−0.50
4241.923	32,778	(e)	2.5	56,346	(o)	1.5				−0.81
4245.845	20,135	(e)	2.5	43,681	(o)	2.5	−1.154		−0.40	−0.41
4321.359	27,285	(e)	1.5	50,419	(o)	1.5				−0.51
4334.640	23,146	(e)	4.5	46,209	(o)	5.5		−0.59	−0.66	−0.74
4350.516	23,146	(e)	4.5	46,125	(o)	4.5				−0.16
4392.055	21,638	(e)	3.5	44,400	(o)	3.5				−0.23
4417.358	15,254	(e)	0.5	37,886	(o)	1.5		−1.00	−0.95	−0.88
4422.715	30,942	(e)	5.5	53,546	(o)	4.5				0.03
4426.173	28,547	(e)	2.5	51,134	(o)	1.5				−0.75
4483.280	32,778	(e)	2.5	55,077	(o)	1.5				−0.88
4486.630	32,778	(e)	2.5	55,060	(o)	2.5				−0.68
4524.699	31,878	(e)	4.5	53,972	(o)	3.5				−0.66
4535.361	21,638	(e)	3.5	43,681	(o)	2.5	−1.133		−0.83	−0.86
4570.683	28,547	(e)	2.5	50,419	(o)	1.5				−0.95
4599.450	28,105	(e)	4.5	49,840	(o)	4.5	−0.504		−0.38	−0.46
4613.717	31,878	(e)	4.5	53,546	(o)	4.5				−0.16
4622.705	20,135	(e)	2.5	41,761	(o)	2.5				−0.77
4675.454	28,458	(e)	3.5	49,840	(o)	4.5	−1.048		−0.74	−0.92
4817.206	21,638	(e)	3.5	42,391	(o)	4.5			−0.72	−0.82
4834.767	37,440	(e)	3.5	58,117	(o)	2.5				−0.86
4865.418	28,458	(e)	3.5	49,006	(o)	2.5				−0.83
4904.511	28,547	(e)	2.5	48,931	(o)	3.5				−0.59
5110.588	32,778	(e)	2.5	52,340	(o)	3.5	−0.908		−0.73	−0.96
5247.128	28,105	(e)	4.5	47,158	(o)	3.5				−0.65
5276.328	37,398	(e)	2.5	56,346	(o)	1.5				−0.87
5346.275	28,458	(e)	3.5	47,158	(o)	3.5				−0.70
5493.239	37,440	(e)	3.5	55,639	(o)	4.5				−0.87
5673.572	37,440	(e)	3.5	55,060	(o)	2.5				−0.58
6027.552	28,105	(e)	4.5	44,691	(o)	3.5				−0.89
6473.888	28,458	(e)	3.5	43,901	(o)	2.5				−0.99
6709.435	37,440	(e)	3.5	52,340	(o)	3.5			−0.98	−0.76

[a] Wavelengths deduced from experimental energy levels. They are given in air for λ longer than 2000 Å and in vacuum for λ shorter than 2000 Å.
[b] Experimental levels from [8,15]. (e) and (o) stand for even and odd parities, respectively.
[c] OSP: oscillator strength parametrization method; HFR+CPOL: pseudo-relativistic Hartree–Fock method with core-polarization corrections (see text).

useful guide for experimenters to perform further spectroscopic measurements in this ion.

Acknowledgments

PP and PQ are respectively Research Director and Research Associate of the Belgian Fund for Scientific Research F.R.S.-FNRS. Financial support from this organization is gratefully acknowledged.

Appendix A. Supplementary material

Supplementary data associated with this article can be found in the online version at http://dx.doi.org/10.1016/j.jqsrt.2015.04.013.

References

[1] Bouazza S, Fienhold M, Guthöhrlein GH, Behrens HO, Dembczynski J. Doppler limited laser spectroscopy on hafnium lines. Part I: Hyperfine structure of even-parity levels. Eur Phys J D 1999;6:303.
[2] Bouazza S, Behrens HO, Fienhold M, Dembczynski J, Guthöhrlein GH. Doppler limited laser spectroscopy on hafnium lines. Part II: Hyperfine structure of odd-parity levels. Eur Phys J D 1999;6:311.
[3] Lundqvist M, Nilsson H, Wahlgren GM, Lundberg H, Xu HL, Jang Z – K, et al. Improved oscillator strengths and wavelengths in Hf II, with applications to stellar elemental abundances. Astron Astrophys 2006;450:407. http://dx.doi.org/10.1051/0004-6361:20054474.
[4] Lawler JE, Den Hartog EA, Labby ZE, Sneden C, Cowan JJ, Ivans II. Improved laboratory transition probabilities for Hf II and hafnium abundances in the sun and 10-metal-poor stars. Astrophys J Suppl Ser 2007;169 [1200049/214/2/18].
[5] Kurucz RL. ⟨http://kurucz.harvard.edu/atoms⟩ [online].
[6] Ruczkowski J, Elantkowska M, Dembczynski J. An alternative method for determination of oscillator strengths: the example of Sc II. J Quant Spectr Radiat Transfer 2014;145:20. http://dx.doi.org/10.1016/j.jqsrt.2014.04.0148.
[7] Wyart JF. Étude systématique des configurations électroniques $(5d+6s)^N$ dans les éléments une fois ionisés du groupe du platine. Opt Pura Y Apl 1977;10:177.
[8] Wyart JF, Blaise J. Configuration mixing in singly-ionized platinum group elements. I. Low odd configurations of Hf II, Ta II and W II. Phys Scr 1990;42:209.
[9] Bouazza S. Investigations of hyperfine structure and isotope shift predictions in Hf II. Int J Quant Chem 2012;112:470. http://dx.doi.org/10.1002/qua.22974.
[10] Cowan RD. The theory of atomic structure and spectra. Berkeley: Berkeley University of California Press; 1981.
[11] Quinet P, Palmeri P, Biémont E, McCurdy MM, Rieger G, Pinnington EH, et al. Experimental and theoretical lifetimes, branching fractions and oscillator strengths in LuII. Mon Not R Astr Soc 1999;307:934.
[12] Quinet P, Palmeri P, Biémont E, Li ZS, Zhang ZG, Svanberg S. Radiative lifetime measurements and transition probability calculations in lanthanide ions. J Alloys Compds 2002;344:255.
[13] Fivet V, Biémont E, Engström L, Lundberg H, Nilsson H, Palmeri P, et al. Radiative lifetime measurements and calculations in doubly ionized tantalum (Ta III). J Phys B: At Mol Opt Phys 2008;41:015702.
[14] Fraga S, Karwowski J, Saxena KMS. Handbook of atomic data. Amsterdam: Elsevier Scientific Publishing Company; 1976.
[15] ⟨http://physics.nist.gov/asd⟩.
[16] Quinet P, Fivet V, Palmeri P, Biémont E, Engström L, Lundberg H, et al. Branching fractions and A-values in singly ionized tanatlum (Ta II). Astron Astrophys 2009;493:711.
[17] Nilsson H, Engström L, Lundberg H, Palmeri P, Fivet V, Quinet P, et al. Lifetime measurements and transition probability calculations in singly ionized tungsten (W II). Eur Phys J D 2008;49:13.
[18] Palmeri P, Quinet P, Biémont E, Xu HL, Svanberg S. Transition probabilities and lifetimes in singly ionized rhenium. Mon Not R Astr Soc 2005;362:1348.
[19] Quinet P, Palmeri P, Biémont E, Jorissen A, Van Eck S, Svanberg S, et al. Transition probabilities and lifetimes in neutral and singly ionized osmium and the solar osmium abundance. Astron Astrophys 2006;448:1207. http://dx.doi.org/10.1051/0004-6361:20053852.
[20] Xu HL, Svanberg S, Quinet P, Palmeri P, Biémont E. Improved atomic data for iridium atom (Ir I) and ion (Ir II) and the solar content of iridium. J Quant Spectrosc Radiat Transfer 2007;104:52.
[21] Quinet P, Palmeri P, Fivet V, Biémont E, Nilsson H, Engström L, et al. Laser-induced-fluorescence lifetime measurements and relativistic Hartree–Fock oscillator strength calculations in singly ionized platinum. Phys Rev A 2008;77:022501.
[22] Fivet V, Quinet P, Biémont E, Xu HL. Transition probabilities and lifetimes in gold (Au I and Au II). J Phys B: At Mol Opt Phys 2006;39:3587.
[23] Ruczkowski J, Bouazza S, Elantkowska M, Dembczynski J. Semi-mpirical analysis of oscillator strengths for Nb II. J Quant Spectrosc Radiat Transfer 2015;155:20. http://dx.doi.org/10.1016/j.jqsrt.2014.12.014.
[24] Bouazza S, Ruczkowski J, Elantkowska M, Dembczynski J. Hyperfine structure, lifetime and oscillator strength studies of V II. J Quant Spectrosc Radiat Transfer 2015, submitted.